



Research Paper

NATURAL CONVECTION FLOW SIMULATION FOR VARIOUS APEX ANGLES IN HEATED PRISMATIC CAVITY

Walid Aich^{1*} and Ahmed Omri¹

*Corresponding Author: Walid Aich, ✉ aich_walid@yahoo.fr

Heat transfer and fluid flow due to buoyancy forces in an isosceles prismatic enclosure using the control-volume finite-element method is carried out for different apex angles. This configuration represents solar energy collectors, conventional attic spaces of greenhouses and buildings with pitched roofs. The bottom is submitted to a uniform heat flux, the two top inclined walls are symmetrically cooled and the two vertical walls are assumed to be perfect thermal insulators. Governing parameters, which are effective on flow field and temperature distribution, are; Rayleigh number, aspect ratio of the enclosure and the apex angle. Streamlines, isotherms, velocity and temperature profiles, local and mean Nusselt numbers are presented. It has been found that a pitchfork bifurcation occurs at a critical Rayleigh number, above which the symmetric solutions becomes unstable and asymmetric solutions are instead obtained. It's also found that the heat transfer decreases with increasing of the apex angle at small Rayleigh number due to quasi-conduction dominant heat transfer regime. At the highest Rayleigh number, the increasing of the apex angle enhances the heat transfer.

Keywords: Natural convection, Apex angle, Aspect ratio, Rayleigh number, Nusselt number, Heat transfer

INTRODUCTION

Buoyancy induced flow and heat transfer is an important phenomenon in engineering systems due to its wide applications such as solar collectors, fire control, studies of air movement in attics and greenhouses, cooling electronic devices and nuclear reactors. Generally, in most of the experimental and numerical

studies, geometrical model is chosen as square or triangular enclosures. However, natural convection in prismatic enclosures is especially important because it is frequently found in attic areas of domestic buildings.

A significant amount of earlier studies involves various applications within triangular cavity. Akinsete and Coleman (1982)

¹ Unité de Recherche Matériaux, Energie et Energies Renouvelables, faculté des sciences, Université de Gafsa, Tunisie.

investigated natural convection in an air-containing long right-triangular enclosure with a height to base ratio from 0.0625 to 1 for Grashof numbers from 800 to 6000. Poulidakos and Bejan (1983) studied the fluid dynamics inside a triangular enclosure with a cold upper wall and a warm horizontal bottom wall. Asymptotic analysis is performed to elucidate theoretically the steady-state circulation flow pattern and temperature field. The transient phenomenon, beginning with the sudden cooling of the upper wall, is considered. Campo *et al.* (1988) used the Galerkin finite element method with a stream function-vorticity-temperature formulation to examine all possible combinations of cold, hot, and adiabatic wall conditions for various Grashof numbers and aspect ratios. Salmun (1994 and 1995) presented convection patterns in a triangular domain and the instability of a single cell in a steady state solution in a triangular enclosure. Asan and Namli (2000a and 2000b) conducted a numerical study of buoyant flow in a roof with a triangular cross-section for two-dimensional laminar natural convection under summer- and winter-day boundary conditions. Their results showed that most of the heat exchange takes place near the intersection of the active walls and that heat transfer decreases with the increasing of aspect ratio. The finite-element method was used by Holtzman *et al.* (2000) to model the complete isosceles triangular cavity without claiming cavity symmetry. These authors performed a flow visualization study to validate experimentally the existence of symmetry-breaking bifurcations in one cavity of fixed aspect ratio. This anomalous bifurcation phenomenon was intensified by gradually increasing the Grashof number. The

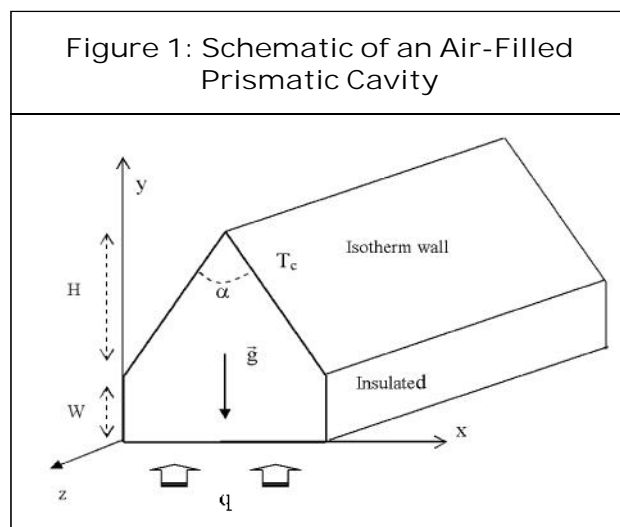
main conclusion drawn in this paper was that, for identical isosceles triangular cavities engaging symmetrical and non-symmetrical assumptions, the differences in terms of mean Nusselt number were about 5%. Omri *et al.* (2005 and 2007) studied laminar natural convection in a triangular cavity with isothermal upper sidewalls and with a uniform continuous heat flux at the bottom. The study showed that the flow structure and the heat transfer are sensitive to the cavity shape and to the Rayleigh number. An optimum tilt angle was determined corresponding to a minimum of the Nusselt number and for a maximum of the temperature at the bottom center. In recent years, there have been increasing research activities in this area (Hajri *et al.*, 2007; Hakan *et al.*, 2007; Koca *et al.*, 2007; and Varol *et al.*, 2007a and 2007b).

The present study deals with the natural convection within prismatic enclosures with a bottom submitted to a uniform heat flux, two top inclined walls symmetrically cooled and two vertical walls assumed to be adiabatic. The entire physical domain is taken into consideration for the computations and no symmetry plane is assumed. This step is necessary for the present problem because, as demonstrated experimentally by Holtzman *et al.* (2000) for the laminar regime analysis, a pitchfork bifurcation occurs at a critical Grashof number, above which the symmetric solutions becomes unstable to finite perturbations and asymmetric solutions are instead obtained. The effect of geometry has been illustrated for various Rayleigh number, aspect ratio and apex angle of the enclosure. Numerical results are presented in terms of isotherms and streamlines along with the local and average

heat transfer rates (Nusselt number). The physical model considered here is shown in Figure 1, along with the important geometric parameters. It consists of a juxtaposition of an upper prismatic space and a lower rectangular cavity. The aspect ratio of the enclosure is defined as $A_w = W/H$. The horizontal bottom is exposed to a uniform heat flux q while the inclined walls are maintained at a constant temperature T_c and the vertical walls are insulated. With this geometry and boundary conditions, the present study reports the computations for cavities at various apex angle, ranging from 30° to 90° , and two particular aspect ratio $A_w = 0.75$ and $A_w = 1$, and their effects on the heat transfer process is analysed. Results are presented in terms of the variation of the local and average Nusselt number at the heated surface. Another important parameter of investigation is the Rayleigh number which is varied from 10^3 to 10^6 .

MATHEMATICAL FORMULATION

The governing equations for two-dimensional, laminar steady incompressible



buoyancy-induced flows with Boussinesq approximation using conservation of mass, momentum and energy in dimensionless form can be written as:

$$\frac{\partial U}{\partial X} + \frac{\partial V}{\partial Y} = 0$$

$$U \frac{\partial U}{\partial X} + V \frac{\partial U}{\partial Y} = -\frac{\partial P}{\partial X} + \left[\frac{\partial^2 U}{\partial X^2} + \frac{\partial^2 U}{\partial Y^2} \right]$$

$$U \frac{\partial V}{\partial X} + V \frac{\partial V}{\partial Y} = -\frac{\partial P}{\partial Y} + \left[\frac{\partial^2 V}{\partial X^2} + \frac{\partial^2 V}{\partial Y^2} \right] + \frac{Ra}{Pr} \theta$$

$$U \frac{\partial \theta}{\partial X} + V \frac{\partial \theta}{\partial Y} = \frac{1}{Pr} \left[\frac{\partial^2 \theta}{\partial X^2} + \frac{\partial^2 \theta}{\partial Y^2} \right]$$

where U and V are, respectively, the velocity components in the X and Y direction; P is the pressure, and θ is the temperature. In the generated set, the temperature is normalized as:

$$\theta = \frac{k.(T - T_c)}{q.H}$$

Distances, velocity components and pressure are normalized by reference respectively to:

$$H, \frac{\epsilon}{H} \text{ and } \frac{\rho.H^2}{\mu.\epsilon^2}$$

The dimensionless height of the triangular part is then equal to unity ($H^* = 1$) and the dimensionless width of the bottom is:

$$L = 2 \tan (\alpha / 2)$$

where q is the value of the thermal flux at the bottom, α is the cover tilt angle and ϵ is the kinematical viscosity.

A Control Volume Finite Elements Method (Baliga, 1978; Baliga and Patankar, 1983; Omri and Ben Nasrallah, 1999; and Omri, 2000) is used in this computation. The domain of interest is divided in triangular elements and a polygonal volume is constructed around each node by joining the element centre with the middle of sides. The set of governing equations is integrated over the Control Volume with use of an exponential interpolation in the mean flow direction and a linear interpolation in the transversal direction inside the finite element. The algebraic equations are then solved by the conjugate gradient Method. Solutions were assumed to converge when the following convergence criteria was satisfied for every variable at every point in the solution Domain.

$$\left| \frac{\{\}_{new} - \{\}_{old}}{\{\}_{new}} \right| \leq 10^{-4}$$

where $\{\}$ represents U, V, P and θ .

DIMENSIONLESS BOUNDARY CONDITIONS

The solution must satisfy dimensionless boundary conditions which are as follows:

- At the cover walls: $U = 0, V = 0$ and $\theta = 0$
- At the vertical walls: $U = 0, V = 0$ and

$$\frac{d\theta}{dn} = 0$$

- At the heated horizontal bottom, an external dimensionless thermal flux density $q' = 1$ is considered with $U = 0, V = 0$.

We define the local heat transfer coefficient at a given point on the heated wall as follows:

$$h_x = \frac{q}{(T(x) - T_c)}$$

where $T(x)$ is the local temperature at this wall. Accordingly the local Nusselt number and the average Nusselt number can be obtained respectively as:

$$Nu = \frac{h_x \cdot L}{k} = \frac{1}{\theta''(x)}$$

$$\overline{Nu} = \frac{\overline{h_x} \cdot L}{k} = \frac{1}{L} \int_0^L \frac{1}{\theta''(x)} dx$$

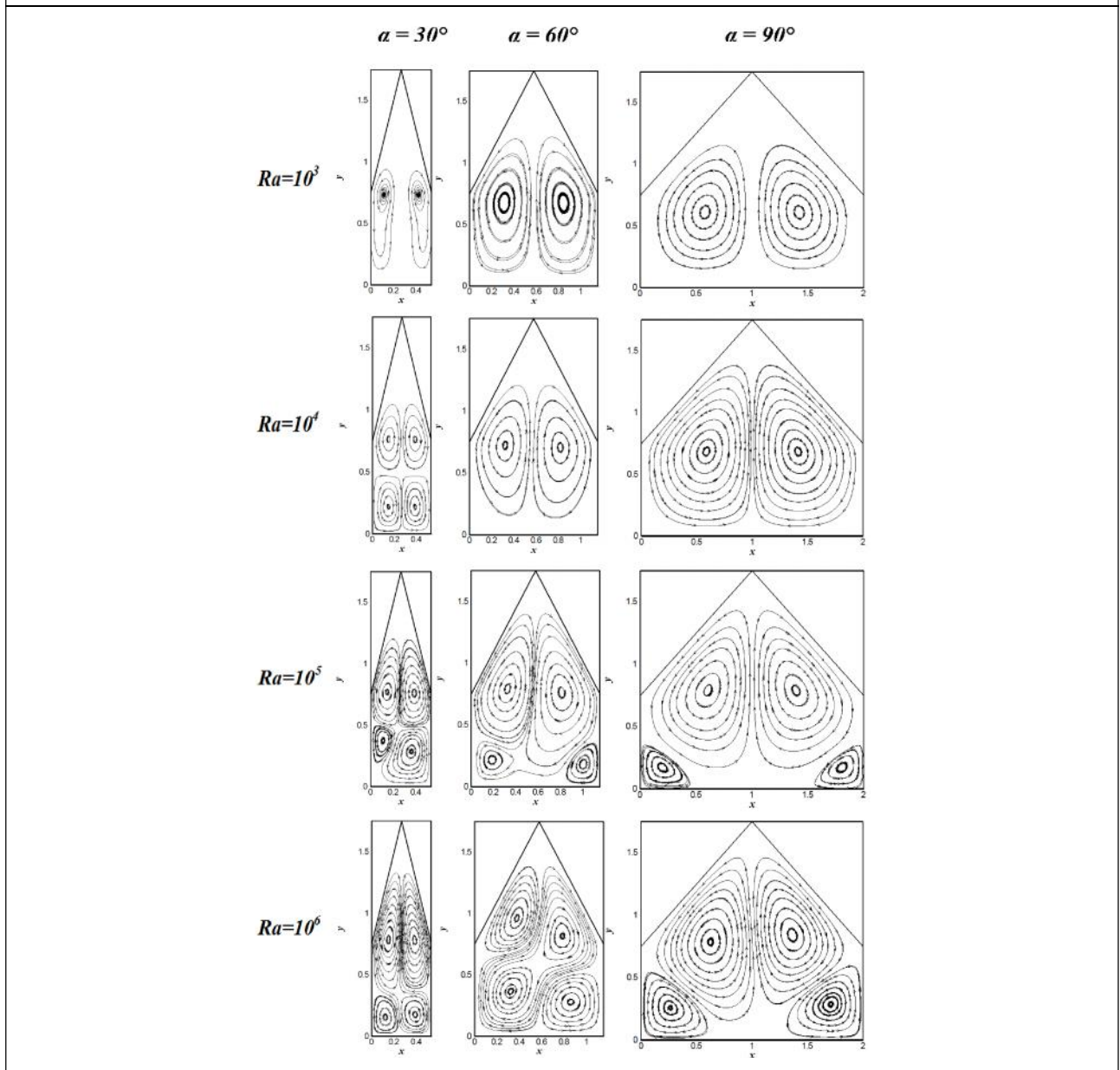
where $\theta''(x)$ is the local dimensionless temperature.

RESULTS AND DISCUSSION

A numerical study has been carried out to simulate temperature and flow fields in a prismatic enclosure heated from below. Prandtl number is taken as 0.71 which corresponds to air. The parameters governing the heat transfer and fluid flow are as follows: the apex angle of the cavity, r from 30° to 90° ; Rayleigh number, Ra from 10^3 to 10^6 and the aspect ratio of the enclosure which takes two particular values $A_w = 0.75$ and $A_w = 1$. Flow field will be shown with streamlines patterns for various combinations of mentioned governing parameters. Temperature field and heat transfer will be presented in terms of isotherms and Nusselt number (local and mean), respectively.

For lower values of Ra ($Ra = 10^3$), as shown in Figures 2 and 3, for each aspect ratio the computed flow is symmetric with respect to the geometric midplane. The flow rises in the center of the enclosure and falls along cold inclined and vertical adiabatic walls creating

Figure 2: Streamlines for $A_w = 0,75$ with Different Apex Angles and Rayleigh Number Values



mirror image structures that rotate clockwise in the right half and counterclockwise in the left half. It is also observed that, for an aspect ratio $A_w = 0.75$, the significant convection is initiated at critical Rayleigh number $Ra = 10^4$ for $r = 30^\circ$ and $Ra = 10^5$ for $r = 60^\circ$ and $r = 90^\circ$. However, for $A_w = 1$, the initiation of the significant effect of convective heat transfer

occurs at $Ra = 10^4$ for each value of the apex angle. For higher values of Ra ($Ra \geq 10^5$), the intensity of convection increases and causes secondary vortex to develop on the lower corners of the cavity. One can see that, by widening the bottom ($r = 90^\circ$) and increasing of Ra , the symmetry of the flow is completely destroyed for an aspect ratio $A_w = 1$ and we

Figure 3: Streamlines for $A_w = 1$ with Different Apex Angles and Rayleigh Number Values

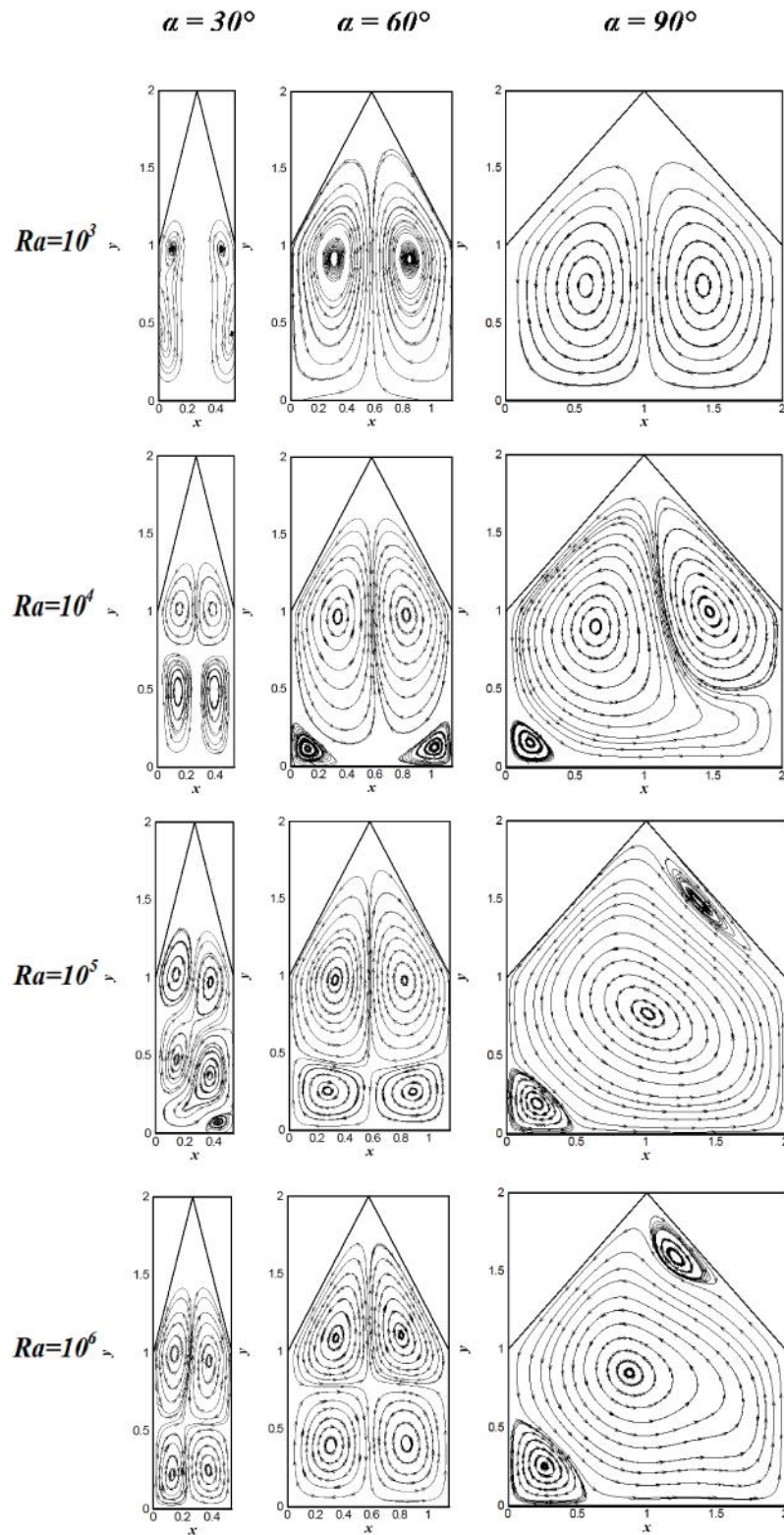
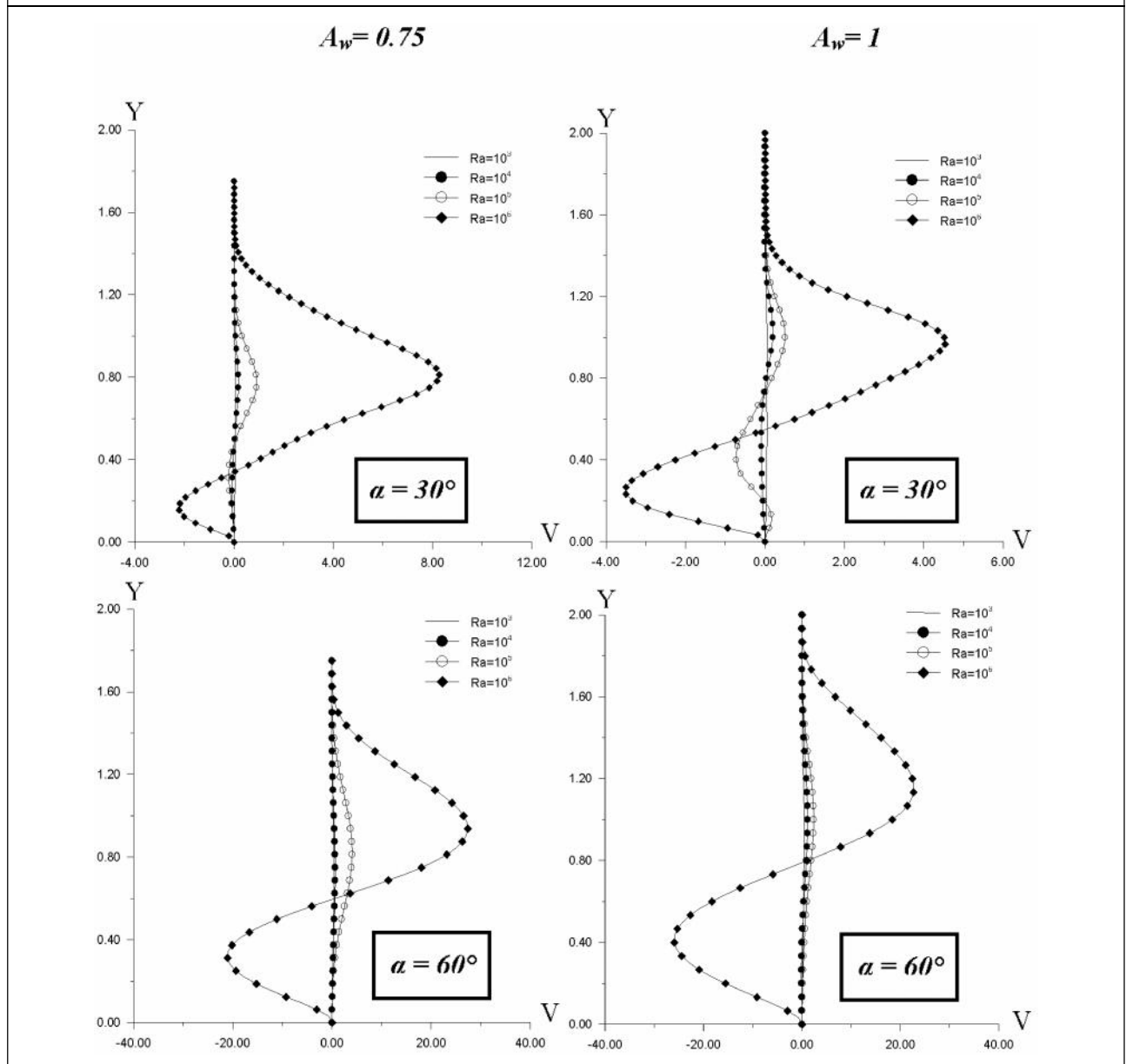


Figure 4: Vertical Velocity Component Profile at the Middle for Different Apex Angles and Rayleigh Number Values



notice the occurrence of pitchfork bifurcation which justifies the choice of considering the entire physical domain for the computations.

Figure 4 represent vertical velocity component profile at the midplane for different configurations. It can be noticed that, for smaller cavities ($r = 30^\circ$ and $r = 60^\circ$), the flow have similar behavior near the center line. In fact,

for higher Rayleigh number ($Ra = 10^6$), the fluid is pushed upward at the center of the upper triangular part of the enclosure and moving downward at the center of the rectangular region.

The evolution of the thermal field with Rayleigh number, for different apex angles and two particular aspect ratios $A_w = 0.75$ and

Figure 5: Isotherms for $A_w = 0,75$ with Different Apex Angles and Rayleigh Number Values

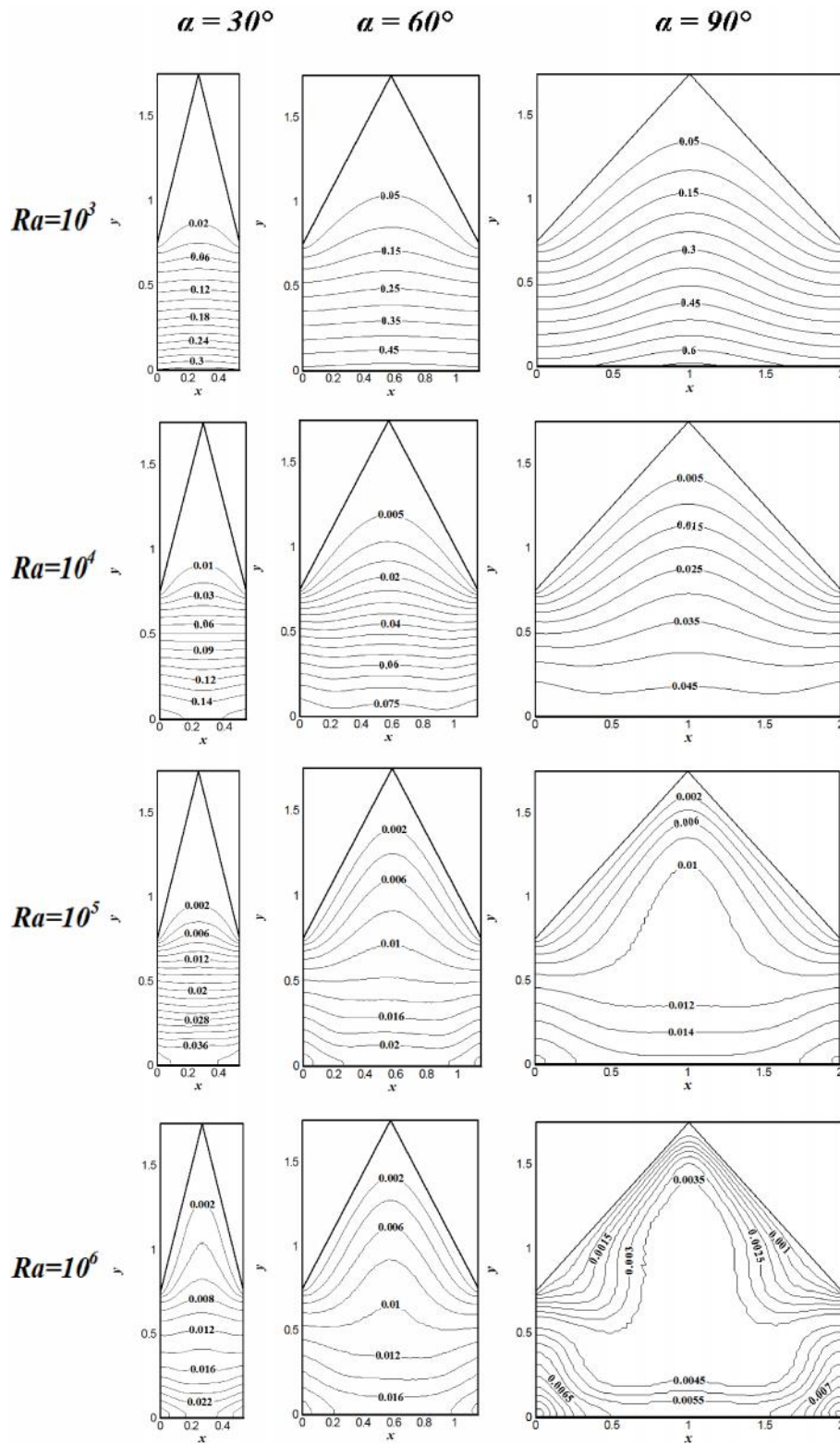


Figure 6: Isotherms for $A_w = 1$ with Different Apex Angles and Rayleigh Number Values

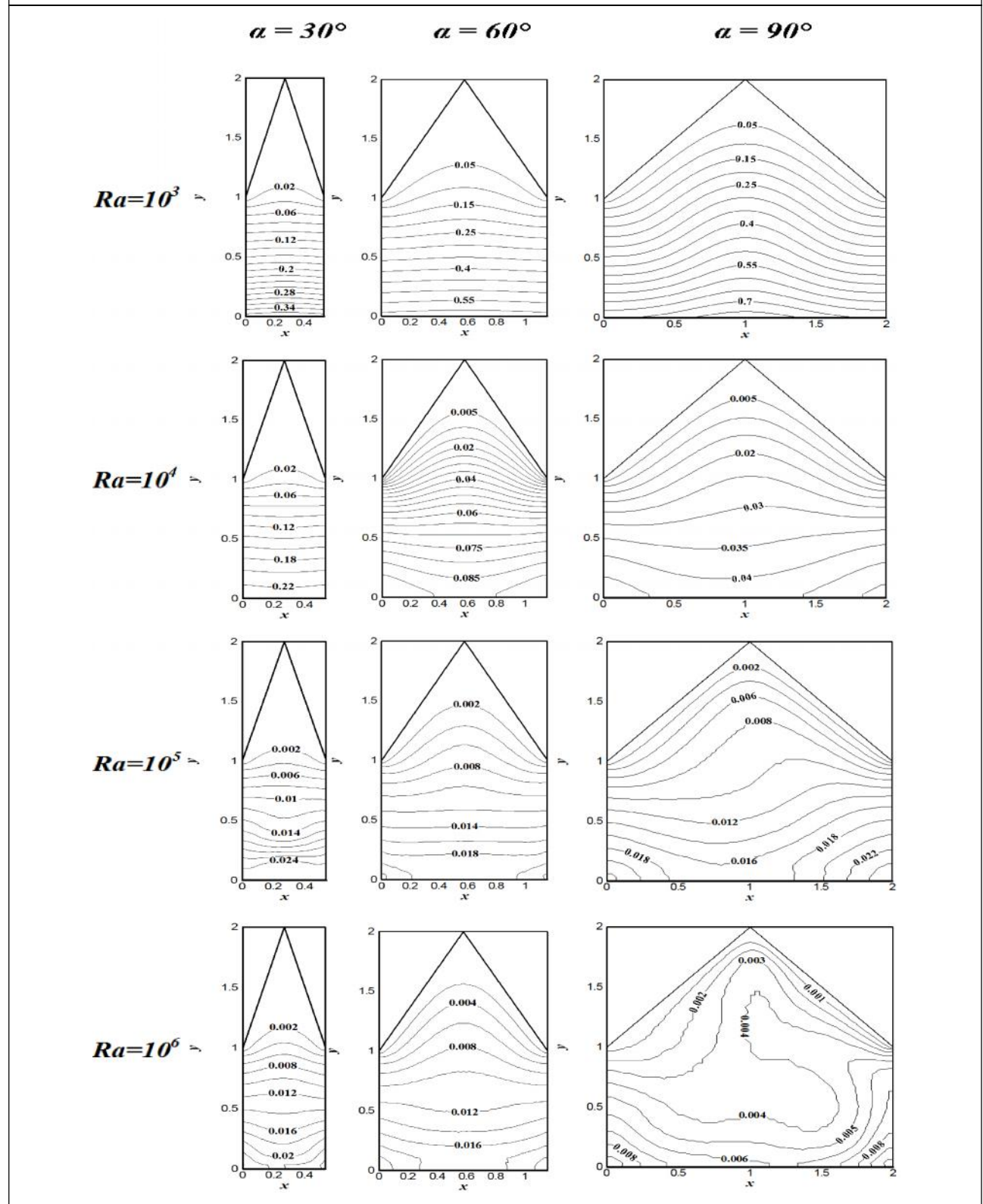
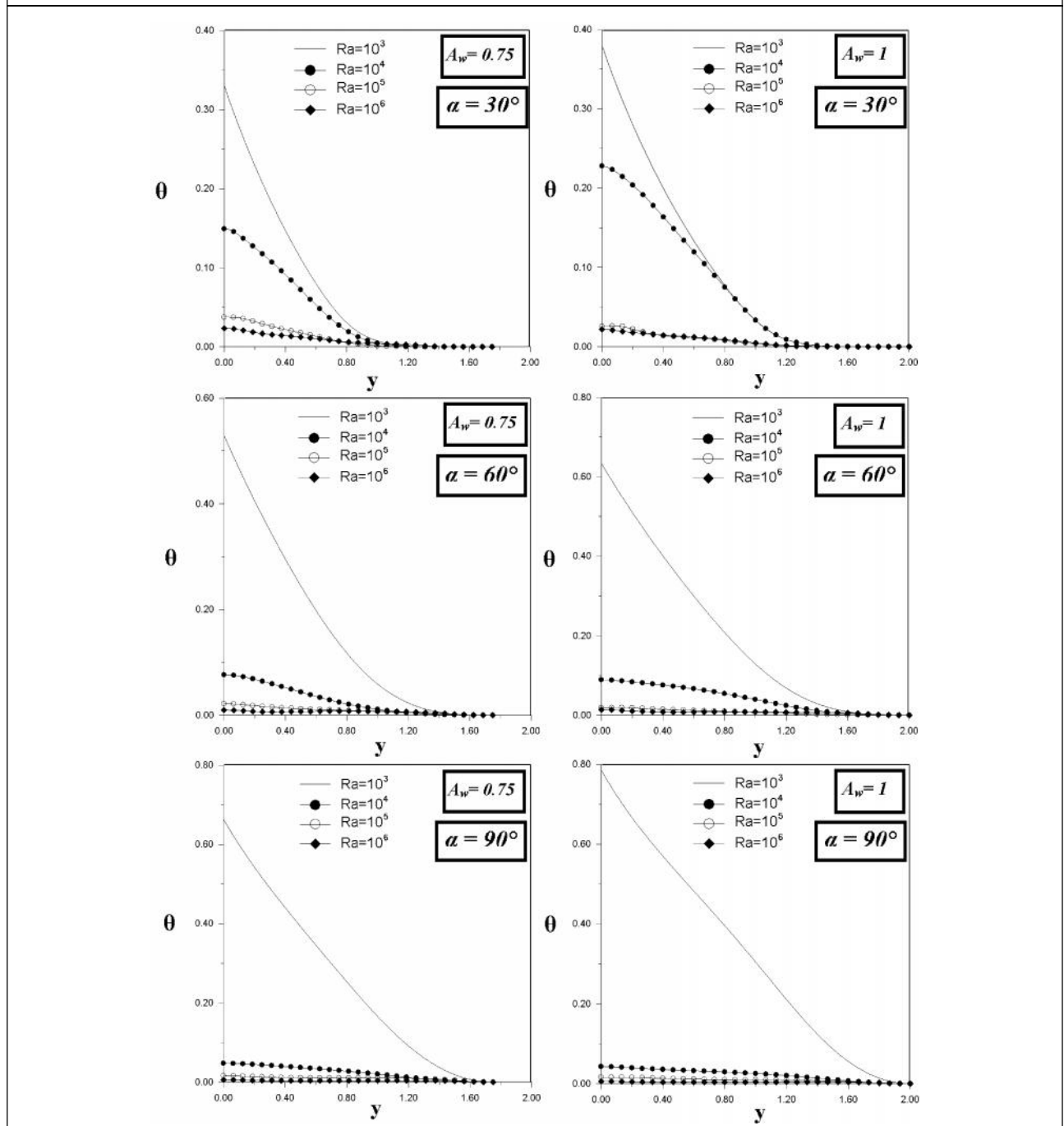


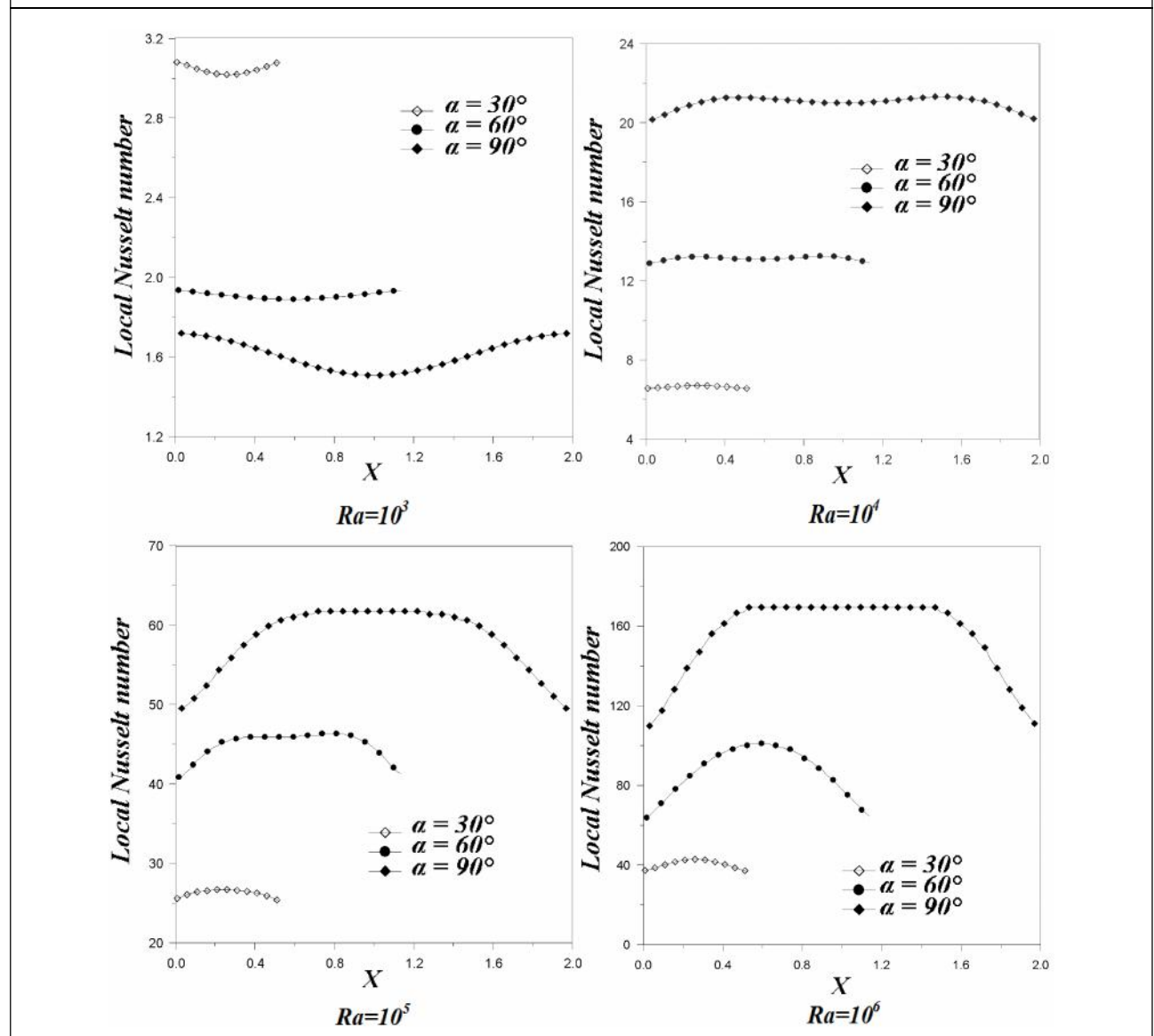
Figure 7: Temperature Profile at the Centreline for Different Apex Angles and Different Values of Rayleigh Number



$A_w = 1$, is presented in Figures 5 and 6, respectively. Isotherms reveal the complexity of the phenomena that take place in spacious cavities ($r = 90^\circ$) at high Ra values. The first remark that can be made concerns the non

uniform distribution of the temperature along the bottom uniformly heated. The second remark concerns the clear absence of stratification in the central region. This indicates that convection effects dominate

Figure 8: Local Nusselt Number at the Heated Bottom for Different Apex Angles and Rayleigh Number Values

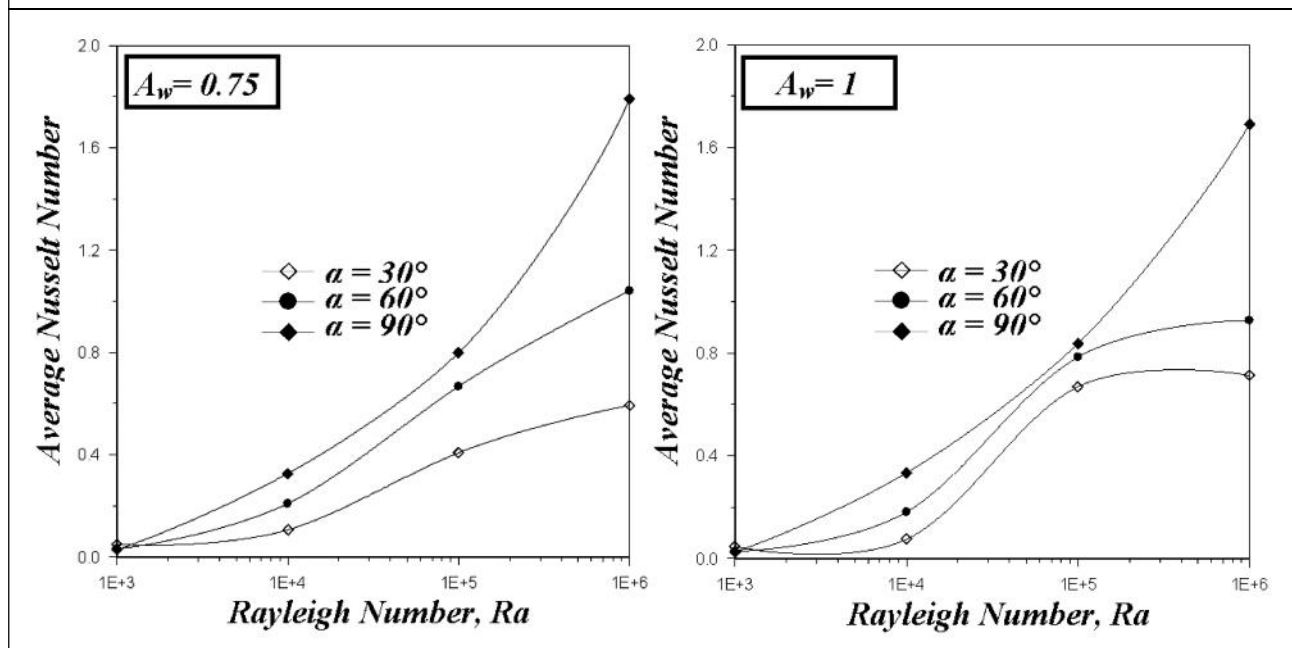


over diffusion effects. Nevertheless, a weak stratification appears only under areas of vortices where a steep vertical temperature gradient leads to stagnation phenomena near the insulated walls which promotes conductive exchange and allows heating of thicker layer where a potentially unstable stratification establishes. Subsequently, the gradually increase in Ra disturbs progressively lower layers, destructs the symmetrical structure and

multiplies recirculation zones which improves the heat transfer and warms well the core of the cavity. Then, the great upper part of the cavity stays cold at a time when the thermal energy received from outside sources locates at the lower layers.

To analyze the thermal field inside, Figure 7 presents the temperature profile at the midplane for various apex angle, different Ra

Figure 9: Variation of the Average Nusselt Number as a Function of Rayleigh Number for Different Apex Angles



values and two particular aspect ratios $A_w = 0.75$ and $A_w = 1$. We have to notice that the flow is characterized by a linear temperature variation in the central region of the cavity. It may also be concluded that the temperature at the bottom ($Y = 0$) decreases at high Ra values. The convection development imposes moving downward of the fluid from the cold upper zone and increases thermal exchange.

The apex angle effects on local Nusselt number at the heated bottom are presented in Figure 8 for different values of Rayleigh number and a particular aspect ratio $A_w = 0.75$. When conduction heat transfer is dominant ($Ra = 10^3$), the variation of the local Nusselt number has the same trend and a minimum value around the bottom centre for all apex angles. Higher heat transfer is obtained for the lower value of the apex angle. However, for the highest Rayleigh number, heat transfer increases with increasing of the apex angle due to increasing of heated surface as

expected. Similar trend of the Nusselt number is observed for an aspect ratio $A_w = 1$ for which the plots are not shown here for brevity. The smallest heat transfer is obtained for the highest aspect ratio due to long distance between hot and cold walls.

Variations of the average Nusselt number as a function of Rayleigh number at the heated bottom, for different apex angles and two different aspect ratios, are presented in Figure 9, It can be seen that the best heat transfer is observed for the highest Rayleigh number, the highest apex angles and smallest aspect ratios.

CONCLUSION

In these analyses, results of the steady-state natural convection heat transfer and flow field inside a prismatic cavity are presented. Governing parameters, which are effective on temperature and flow field, are the Rayleigh

number, the apex angle and the aspect ratio of the enclosure. In view of the obtained results, following findings may be summarized:

- Multiple circulation cells were obtained at the highest Rayleigh number and a pitchfork bifurcation occurs due to stronger convection effects. The symmetrical structure of the flow is completely destroyed even under symmetrical boundary conditions.
- Flow and temperature fields are strongly affected by the apex angle and the aspect ratio of the enclosure and Rayleigh number play an important role on them.
- When conduction is the dominating heat transfer mechanism ($Ra = 10^3$), the variation of the local Nusselt number has the same trend and a minimum value around the bottom centre for all apex angles. Higher heat transfer is obtained for the lower value of the apex angle. However, for the highest Rayleigh number, heat transfer increases with increasing of the apex angle due to increasing of heated surface.
- The smallest heat transfer is obtained for the highest aspect ratio due to long distance between hot and cold walls.
- The best heat transfer is observed for the highest Rayleigh number, the highest apex angles and smallest aspect ratios. 🌀

ACKNOWLEDGMENT

The authors would like to express their deepest gratitude to Mr Ali AMRI and his institution "The English Polisher" for their meticulous and painstaking review of the English text of the present paper.

REFERENCES

1. Akinsete V A and Coleman T A (1982), "Heat Transfer by Steady Laminar Free Convection in Triangular Enclosures", *Int. J. Heat Mass Transfer*, Vol. 25, No. 7, pp. 991-998.
2. Asan H and Namli L (2000a), "Laminar Natural Convection in a Pitched Roof of Triangular Cross-Section: Summer Day Boundary Conditions", *Energy and Building*, Vol. 33, pp. 69-73.
3. Asan H and Namli L (2000b), "Laminar Natural Convection in a Pitched Roof of Triangular Cross-Section Under Winter Day Boundary Conditions", *Energy and Building*, Vol. 33, pp. 753-757.
4. Baliga B R (1978), "A Control-Volume Based Finite Element Method for Convective Heat and Mass Transfer", Ph.D. Thesis, University of Minnesota, Minneapolis, USA.
5. Baliga B R and Patankar S V (1983), "A Control Volume Finite-Element Method for Two-Dimensional Fluid Flow and Heat Transfer", *Numerical Heat Transfer*, Vol. 6, pp. 245-261.
6. Campo *et al.* (1988), "Analysis of Laminar Natural Convection in a Triangular Enclosure", *Numerical Heat Transfer*, Vol. 13, pp. 353-372.
7. Hajri *et al.* (2007), "A Numerical Model for the Simulation of Double-Diffusive Natural Convection in a Triangular Cavity Using Equal Order and Control Volume Based on the Finite Element Method", *Desalination*, Vol. 206, pp. 579-588.

8. Hakan *et al.* (2007), "Laminar Natural Convection Heat Transfer in a Shed Roof with or Without Eave for Summer Season", *Applied Thermal Engineering*, Vol. 27, pp. 2252-2265.
9. Holtzman *et al.* (2000), "Laminar Natural Convection in Isosceles Triangular Enclosures Heated from Below and Symmetrically Cooled from Above", *J. Heat Transfer*, Vol. 122, pp. 485-491.
10. Koca *et al.* (2007), "The Effects of Prandtl Number on Natural Convection in Triangular Enclosures with Localized Heating from Below", *International Communications in Heat and Mass Transfer*, Vol. 34, pp. 511-519.
11. Omri (2000), "Etude de la convection mixte à travers une cavité par la méthode des volumes de contrôle à base d'éléments finis", Thèse de Doctorat, Faculté des Sciences de Tunis, pp. 1-184.
12. Omri A and Ben Nasrallah S (1999), "Control Volume Finite Element Numerical Simulation of Mixed Convection in an Air-Cooled Cavity", *Numerical Heat Transfer*, Vol. 36, pp. 615-637.
13. Omri *et al.* (2005), "Natural Convection Effects in Solar Stills", *Desalination*, Vol. 183, pp. 173-178.
14. Omri *et al.* (2007), "Numerical Analysis of Natural Buoyant induced Regimes in Isosceles Triangular Cavities", *Numerical Heat Transfer, Part A*, Vol. 52, pp. 661-678.
15. Poulidakos D and Beja A (1983), "The Fluid Dynamics of an Attic Space", *J. Fluid Mech.*, Vol. 131, pp. 251-269.
16. Salmun H (1994), "The Stability of a Single-Cell Steady-State Solution in a Triangular Enclosure", *Int. J. Heat Mass Transfer*, Vol. 38, No. 2, pp. 363-369.
17. Salmun H (1995), "Convection Patterns in a Triangular Domain", *Int. J. Heat Mass Transfer*, Vol. 38, No. 2, pp. 351-362.
18. Varol *et al.* (2007a), "Natural Convection Heat Transfer in Gambrel Roofs", *Building and Environment*, Vol. 42, pp. 1291-1297.
19. Varol *et al.* (2007b), "Natural Convection in Triangular Enclosures with Protruding Isothermal Heater", *International Journal of Heat and Mass Transfer*, Vol. 50, pp. 2451-2462.

APPENDIX

Nomenclature

a	- thermal diffusivity, $a = K/(...1C_p)$, [m^2s^{-1}]
A_w	- aspect ratio, $A_w = W/H$, [-]
C_p	- specific isobaric heat capacity, [$JKg^{-1}K^{-1}$]
g	- gravitational acceleration, [ms^{-2}]
H	- height of inclined walls, [m]
H'	- dimensionless height of inclined walls, [-]
K	- thermal conductivity, [$Wm^{-1}K^{-1}$]
Nu	- Nusselt number, [-]
P	- dimensionless pressure, [-]
Pr	- Prandtl number, [-]
q	- thermal flux density, [Wm^{-2}]
q'	- dimensionless thermal flux density, [-]
Ra	- Rayleigh number, $Ra = g.s.q.H^3/(K.a.n)$, [-]
U, V	- dimensionless velocity components in the X and Y directions, [-]
W	- height of vertical walls, [m]
X, Y	- horizontal and vertical dimensionless coordinates, [-]
r	- inclination angle of roofs, $r = 90^\circ$
s	- coefficient of volumetric thermal expansion, [K^{-1}]
\dots	- fluid density, [Kgm^{-3}]
ϵ	- kinematic viscosity, [m^2s^{-1}]
θ	- dimensionless temperature, [-]